Fuel Processing Technology 292 (2026) 108582

Contents lists available at ScienceDirect

Fuel Processing Technology

journal homepage: www.elsevier.com/locate/fuproc

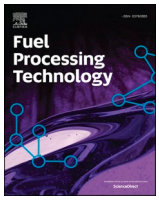

Kaolin as a fuel additive: Influence on gaseous and particulate matter emissions in an industrial-scale biomass CHP unit

Theresa Siegmund *, Lena Schultheiß, Martin Kaltschmitt

Institute of Environmental Technology and Energy Economics, Hamburg University of Technology (TUHH), Eissendorfer Strasse 40, 21073 Hamburg, Germany

ARTICLE INFO

Keywords:
Biomass CHP
Grate firing
(Fuel) additivation
Aluminosilicate
Particulate matter
Carbon monoxide

ABSTRACT

Biomass combustion for carbon-neutral heat and electricity can provide baseload power independent of fluctuations typical for other energy systems (e.g., wind and solar). However, EU emission regulations for biomass-fired CHP units are strict and will likely become more challenging. Fuel-related measures for emission reduction thus complement primary and secondary measures while also addressing corrosion and slagging. Kaolin, a kaolinite-rich aluminosilicate additive, binds alkali metals such as K to form stable potassium aluminosilicates. This reduces gas-phase K compounds that contribute to particulate matter formation, inhibit CO oxidation, and corrosion in flue gas pathways. Lab and small-scale experiments show substantial total particulate matter (TPM) and CO mitigation during kaolin-additivated combustion tests, though large-scale CHP studies remain limited. This study presents results from field trials in a 26 MW_{th} grate-fired biomass CHP using untreated wood chips from residual forest wood and short rotation coppice. Despite variations in fuel input and plant conditions within the measurement campaigns, trials with kaolin dosing of up to 1.0 wt%, showed up to 73% lower K amounts in the flue gas, 91% lower CO, and 39% lower TPM emissions.

1. Introduction

Controlling and reducing airborne emissions from the combustion of solid biofuels to generate heat and/or electricity is a challenge within both small- and large-scale furnaces. Primary control measures – including plant design, the design of the combustion chamber, sufficient insulation, and optimized operating parameters such as staged air supply, fuel staging, air-fuel ratio adjustment, and draft control – offer some mitigation potential [1–3]. However, in many cases, these steps alone are insufficient to meet increasingly stringent environmental regulations. Thus, in large-scale biomass combined heat and power (CHP) facilities, a variety of secondary measures are commonly implemented to comply with legal emission standards. These flue gas treatment systems include particulate matter (PM) removal technologies such as cyclones, electrostatic precipitators, and/or fabric filters, alongside systems aiming for gaseous pollutant reduction, for example, selective catalytic or non-catalytic reduction (SCR, SNCR) for nitrogen oxides (NO_x) and the use of adsorbents like limestone for sulfur dioxide (SO_2) capture [4]. In addition to downstream flue-gas treatments, fuel-side measures targeting the chemical properties of solid biofuels represent another promising route to optimize combustion behavior and directly control emission formation within the combustion chamber. Although pre-treatment methods that chemically alter the fuel (e.g., leaching or pre-drying) tend to be economically impractical for large-scale operations under commercial circumstances, additive strategies that directly incorporate minerals into the biomass fuel have shown notable effects. While such measures have mainly been investigated in small-scale furnaces, significant reductions in airborne emissions and fuel-related operational issues (e.g., slagging, agglomeration, deposit formation, and corrosion) have been reported [5,6].

During the combustion of solid biofuels, alkali metals naturally present within the biogenic material are released as volatile gaseous compounds (e.g., potassium hydroxide (KOH), potassium chloride (KCl), potassium sulfate (K_2SO_4)) into the surrounding gas phase. Upon cooling of the flue gas before release into the atmosphere, these gaseous chemical compounds nucleate from the gas into the solid phase and may further agglomerate. These effects result in the formation of particulate matter (PM) emissions, which can additionally contribute to fouling and corrosion. For example, KCl can promote alkali-chloride-induced corrosion by forming iron chlorides through direct reactions with iron in low-alloyed steels [7]. In addition to particulate matter formation, gaseous K compounds (e.g., KCl and K_2SO_4) interfere with radical-driven

* Corresponding author.
E-mail address: theresa.siegmund@tuhh.de (T. Siegmund).

https://doi.org/10.1016/j.fuproc.2026.108582
Received 1 April 2026; Received in revised form 3 September 2026; Accepted 7 September 2026
Available online 12 September 2026

oxidation reactions (e.g., with hydroxyl ($^{\bullet}OH$) and hydrogen ($H^{\bullet}$) radicals) within the combustion zone, inhibiting carbon monoxide (CO) oxidation.

Among various mineral additives, kaolin – a clay mineral primarily composed of kaolinite ($Al_2Si_2O_5(OH)_4$) – has been extensively studied [5]. Under the conditions prevailing within the combustion zone of a biomass-fired boiler, kaolin/kaolinite reacts with inorganic (alkali) components such as K by forming temperature-stable potassium aluminosilicates (e.g., kalsilite ($KAlSiO_4$) and leucite ($KAlSi_2O_6$)), accumulating within the bottom ash [6,8]. The result is reduced carbon monoxide (CO) and total particulate matter (TPM) emissions (Fig. 1). This has been demonstrated in laboratory-scale experiments and small-scale combustion tests [9–13]. For large-scale units, such reductions could translate into a decreased particle load on (fabric) filters, lower equipment erosion and abrasion, improved operational efficiency, and a more easily achievable compliance with legal emission standards. Additional synergies, particularly in long-term application, could arise from these effects, such as a more reliable operation due to fewer slagging issues, extended maintenance intervals for the plant and (fabric) filters due to lower corrosion tendencies and lower particulate matter levels, and changes in ash and slag quality and amounts relevant for disposal and/or further use. Such approaches may be especially of interest in facilities that utilize (alternative) biomass feedstocks, including agricultural residues (e.g., straw), demolition wood, and waste wood. Nevertheless, data regarding the application of additives such as kaolin in grate-fired combustion units larger than 1 MW_{th} remain limited. Available investigations often focus on circulating fluidized bed (CFB) boilers operating under different conditions and having distinct fuel additive requirements compared to grate-fired systems [14–16]. Initial promising results on the use of additives for particulate emission reduction in large-scale grate-fired boilers have been reported from a Danish biomass boiler fueled with straw (100 MW_{th}) [17]. In addition, studies exploring the influence of fuel additivation on deposit formation, such as on heat exchanger surfaces, have been conducted in a Danish pulverized fuel boiler (250 MW_{th}) combusting ground straw pellets [18].

Against this background, this work investigates the effects of kaolin fuel additivation on emissions and ash chemistry in a large-scale grate-fired combustion system using solid woody biofuels. Additivation trials were conducted at different loads and kaolin concentrations in a biomass-fired CHP unit (up to 26 MW_{th}) with a fuel mixture consisting of residual forest wood and short rotation coppice wood chips. Particular focus during these trials was on the reduction of total particulate matter upstream of secondary cleaning, the reduction of CO emissions at the stack, as well as shifts of K from the gas phase into the bottom ash.

2. Materials and methods

2.1. Power plant

Fig. 2 shows a schematic drawing of the 26 MW_{th} grate-fired biomass CHP unit, subject to the requirements of the German 44th BImSchV [19] and equipped with an SNCR system (dosing urea), a multicyclone, and fabric filters for secondary flue gas treatment. Wood chips are transported from a fuel bunker to the combustion chamber, where they fall onto a moving grate. The fuel is transported over the grate, and bottom ash (BA) is removed via a wet ash-removal system at the end of the grate. Combustible gases rise and flow through three flue gas ducts to the economizer, where a mobile measuring device was located for reference values in targeted measurements during the kaolin additivation trials in addition to the stationary and permanently operated measuring points of the plant needed to fulfill the legal requirements. After the economizer, the flue gas passes through a cyclone and a fabric filter, before the filtered flue gas is released into the atmosphere via the stack. During additivation trials, kaolin was added using a steel big bag hanger connected to a tube chain conveyor (TRK 115, Horstkötter). The additive was transported to the fuel bunker, where the powder was distributed across the fuel on the inclined conveyor, before it was fed into the combustion chamber. The speed of the additive tube chain conveyor was controlled via power output, and the conveyor was coupled to the inclined conveyor for fuel transport to the boiler; i.e., additive addition occurred only during simultaneous fuel transport. Within the plant, continuous measurements of steam input, air-fuel ratios, temperatures, differential pressure in the cyclone and fabric filters, as well as the volume flow and chemical composition of the flue gas stream, were recorded.

2.2. Fuel and additive

A wood chip fuel blend from residual forest wood and short rotation coppice was used as a solid fuel within the combustion unit. For each measurement trial, fuel samples were collected and analyzed. As an additive, the aluminum-silicate-based mineral kaolin, consisting mainly

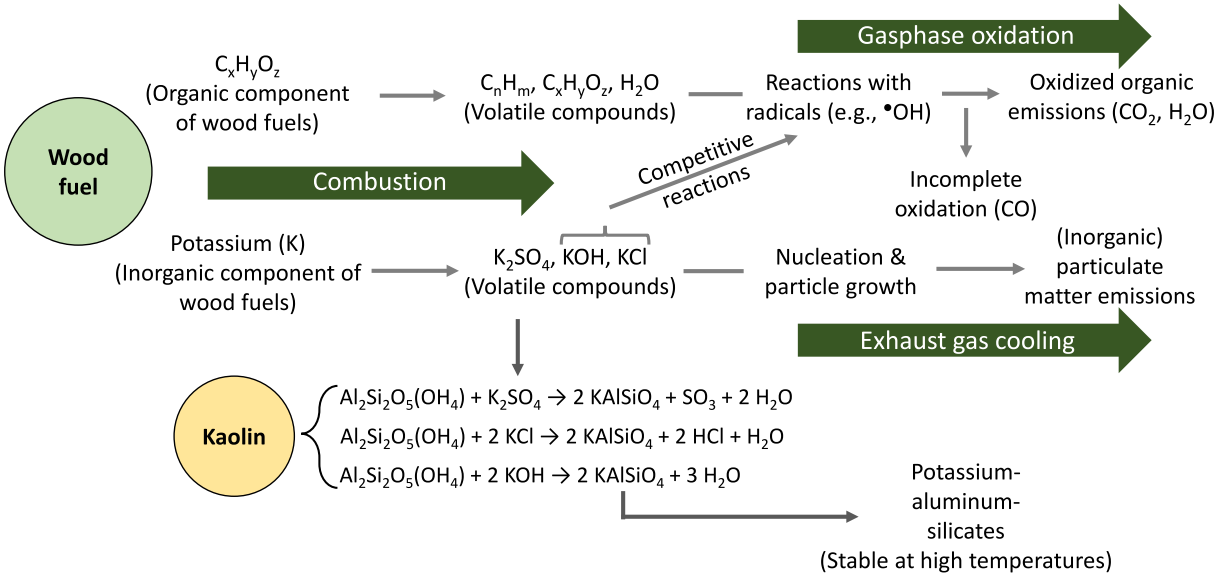

Fig. 1. Thermo-chemical conversion of biomass on the formation pathway of inorganic particulate matter (PM) from potassium (K) and formation of carbon monoxide (CO) emissions, as well as the effect of kaolin additivation leading to reduced inorganic PM and CO emissions.

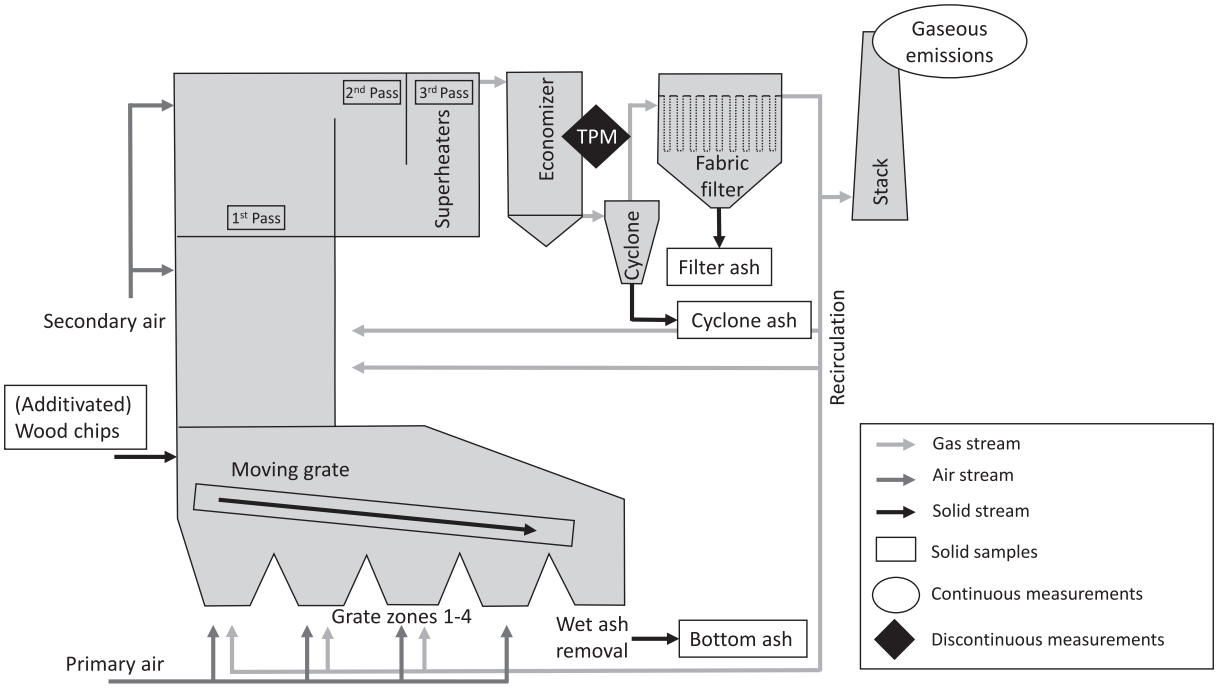

Fig. 2. Schematic overview of biomass combined heat and power (CHP) unit with gas, air, and solid streams, solid samples for subsequent analyses and the location for targeted total particulate matter (TPM) measurements before secondary flue gas cleaning system and measurements of gaseous emissions at the stack.

of kaolinite ($Al_2Si_2O_5(OH)_4$), was used. The mineral additive was supplied in 300 kg big bags (Gebrüder Dorfner Kaolin und Kristallquarzsandwerke) as milled "Kaolin FP 80". The properties of the additive are listed in Table 1.

2.3. Measurements

Six two-day measurement campaigns were conducted, resulting in nine separate measurement trials with different amounts of kaolin added within a specified time frame. An overview of the campaigns and the resulting trials with respective mean values during measurement and daily values (provided by the plant operators) is shown in Table 2. The measurement campaigns include reference measurements conducted for two days (Ref_FL, Ref_PL_a, Ref_PL_b) and measurements with different kaolin concentrations (one day per trial and concentration), of which the trials K_FL_0.3 and K_FL_0.8a, K_FL_0.8b and K_FL_1.0, K_PL_0.5 and K_PL_0.8 were carried out on consecutive days, respectively (refer to the months in Table 2). The total duration of continuous additivation in a trial was 4 to 7 h. Biomass and bottom ash samples were taken after the start of the additivation and after the last total particulate matter measurement (see Section 2.3.1). Total particulate matter measurements were conducted only during additivation, while the first particulate matter sampling was conducted not earlier than 20 min after the start of kaolin additivation, to ensure that the additivated fuel had reached the combustion chamber and the additive could take effect. Cyclone ash was collected at the end of each of the six measurement campaigns and is therefore not available for every dosage trial. The measurement period of a trial for the evaluation of the continuously measured gaseous emissions is defined as the period of additivation plus 1 h to account for the plant's inertia. The additive concentration in the solid biofuel was calculated retrospectively based on average additive consumption and the amount of fuel burned, and ranged from 0.3 to 1.0 wt%. From the average K concentration from the biofuel in the respective trials (Section 3.1) and the additive content, the molar kaolin to K ratio was calculated. Theoretically, for a complete incorporation of K from the fuel by kaolin, a minimum molar kaolin to K ratio of 0.5 is necessary. The trials were classified as full load (FL, median steam load: 29.8 to 32.6 t/h) and partial load (PL, median steam load: 20.4 to 28.3 t/h) operations.

Table 1
Properties and chemical composition of kaolin additive [20].

Parameter	Unit	Kaolin FP 80
Bulk density	kg/m^3	250–350
Density	g/cm^3	ca. 2.6
Specific surface area	m^2/g	ca. 8
Particle size	µm	<20
SiO_2	wt%	48.3
Al_2O_3	wt%	36.0
Fe_2O_3	wt%	0.5
K_2O	wt%	2.1

2.3.1. Solid samples (biomass, total particulate matter, and ashes)

The gravimetric determination of total particulate matter emissions was carried out using a manual, discontinuous measurement principle in accordance with DIN EN 13284-1 [32] and VDI 2066-1 [33], sampling a partial flue gas stream passing the economizer for 5 min each. The flue gas was passed through an out-stack filter unit (Paul Gothe) with previously at 180 °C baked-out quartz filters with a diameter of 45 mm and a particle retention capacity of 0.3 µm (MACHEREY-NAGEL). Samples were taken back-to-back, with a total amount of 15 to 39 filters each measurement trial. After sampling, the filters were reheated and reweighed, and the concentration related to an oxygen reference concentration of 6 vol% in order to correct for dilution effects. This was done by multiplying the measured concentration for dry flue gas and standard conditions by the correction factor f_c. The reference (*ref*) oxygen concentration and the measured (*m*) oxygen concentrations are represented as o_{ref} and o_m, respectively. Potential outliers were identified using the 1.5-IQR rule and removed from the dataset.

$$f_c = (21\% - o_{ref}) / (21\% - o_m)$$

(Additivated) Biomass from the inclined conveyor as well as bottom ashes (BA) were collected before and after total particulate matter sampling each day during the measurement campaigns; thus, for each kaolin trial, two samples were collected. Cyclone ash (CA) was collected

Table 2
Overview of conducted measurements with (K_) and without (Ref_) the addition of kaolin in different concentrations of 0.3 wt% (_0.3) till 1.0 wt% (_1.0) in a 26 MW_{th} biomass combined heat and power (CHP) unit at full load (FL) and partial load (PL). The molar kaolin to potassium (K) ratio was calculated based on average K content of biomass (BM) samples from respective trials.

		During measurement				Daily average			Number of samples			
Campaign #	Abbreviation of trial	Kaolin	Molar kaolin to K ratio	Mean steam load	Classification	Boiler output	Fuel Input	LHV of fuel	Biomass	Bottom ash	Cyclone ash	Month
		wt%	$mol_{kaolin}/mol_{K,BM}$	t/h		MW_{th}	t/h	MJ/kg				
1	Ref_FL	–	0	30.0	Full load	24.6	11.8	8.6	2	2	1	January 2025
2	K_FL_0.3	0.3	0.4	32.4	Full load	25.8	10.5	10.2	2	2		March 2025
2	K_FL_0.8a	0.8	1.2	32.0	Full load	25.7	10.8	9.8	2	2	1	March 2025
3	K_FL_0.8b	0.8	1.1	29.8	Full load	24.8	9.3	11.0	2	2		May 2025
3	K_FL_1.0	1.0	1.1	29.3	Full load	24.2	8.7	11.5	2	2	1	May 2025
4	Ref_PL_a	–	0	28.4	Partial load	22.8	8.4	11.2	2	2	1	April 2024
5	Ref_PL_b	–	0	20.1	Partial load	17.0	5.6	12.4	2	2	1	August 2024
6	K_PL_0.5	0.5	0.8	25.8	Partial load	18.4	6.7	11.3	2	2		April 2025
6	K_PL_0.8	0.8	1.2	27.2	Partial load	20.7	7.7	11.1	2	2	1	April 2025

at the end of the campaign on the second day, resulting in cyclone samples for the reference trials, as well as 0.8 and 1.0 wt% for full load and 0.8 wt% kaolin additivation for the partial load trial.

Water and ash content. Water content of biofuel samples was determined in a minimum of triplicate in accordance with DIN EN ISO 18134-2 [21] at 105 °C overnight. The ash content of the solid biofuel was determined according to DIN EN ISO 18122 [22] at 550 °C in a muffle furnace (L 40/11 BO, Nabertherm). Before ashing, biomass was pulverized in a cutting mill (SM 200, RETSCH).

Chemical composition. The elemental composition in terms of K, Na, Al, Ca, Mg, and Fe of the total particulate matter (minimum three filters), the ashes, and biomass samples was determined via two-step acid digestion in a microwave, followed by atomic absorption spectroscopy (AAS, contrAA 700, Analytik Jena) measurements in accordance with DIN 22022–1 [23] and DIN EN ISO 16967 [21]. Water-soluble chloride (Cl^-) and sulfate (SO_4^{2-}) ions were measured using ion chromatography (IC, Dionex Sodron ICS-90, Thermo Fisher) according to DIN EN ISO 10304-1 [24].

XRD phase analysis. Crystalline phase analyses of the bottom ash were performed using X-ray diffraction (XRD, D500, Siemens) with Cu Kα radiation at 30 mA and 40 kV. Step scanning was conducted over a range of 3° to 63°, and the resulting diffractograms were analyzed using a reference database (Bruker, EVA software). Prior to analysis, the samples were crushed in a mortar.

2.3.2. Plant operation parameters and gaseous emissions

In addition to the steam load, temperatures at the grate and in the flue gas ducts, as well as pressures in the cyclone, fabric filter, and other plant components, were monitored. Gaseous emissions (i.e., SO_2, NO, NO_2, CO, NH_3, O_2, and H_2O) were measured using the plant's integrated analysis system (ACF-NT, ABB Asea Brown Boveri) at the stack. These data were provided as 10 min averages with a reference oxygen content of 6 vol%. Boxplot of gaseous emissions include measured data from the respective trials, i.e., data from 4 to 7 h. In addition to the permanently installed stationary plant measurement devices in the plant and at the stack in the case of gaseous emissions, a mobile flue gas analyzer (MGAprime Q, MRU) was set up at the economizer during the respective measurement campaigns, to obtain live data for gaseous emissions in 10 s resolution at the total particulate matter sampling point for reference calculation. The O_2 concentration within the flue gas was determined using a paramagnetic or electrochemical sensor.

3. Results and discussion

3.1. Fuel properties

For each trial, two biomass samples were collected. The additivated biomass was transported from the fuel bunker to the combustion chamber via an inclined conveyor, from which it falls onto the grate.

The collection point of the fuel samples was at the highest point of the inclined conveyor and just before the drop point into the combustion chamber. The first sample (a) was taken before the start of the total particulate matter measurements at the economizer (after the start of additivation, if applicable), and the second (b) after the final total particulate matter measurement at the economizer.

Water content. The moisture content of the fuel significantly influences combustion behavior, as higher moisture reduces the heating value, lowers the combustion temperature, and can thus promote the formation of CO and other products of incomplete combustion [25]. Fig. 3 shows the water content of the wood chips combusted in the CHP plant ranging from 29 wt% (K_FL_1.0 sample b) to 48 wt% (Ref_FL sample b). The highest water content was observed in the full-load reference case conducted in January, while the lowest values were measured in May (K_FL_0.5 sample b and K_FL_1.0 sample b). The variation in moisture content correlates with seasonal conditions (see, e.g., [26,27]) and is attributed to differences in precipitation, air humidity, and ambient temperatures. The differences between samples a and b were minor for all trials, as well as the differences between the respective measurement campaigns (e.g., between K_FL_0.3 and K_FL_0.8 a, refer to Table 2), suggesting comparable biofuel properties specifically within these trials. For the partial load trials (_PL_), the moisture contents were generally more comparable.

Ash content. The ash content of the solid biofuel is depicted in Fig. 4. The measured ash content ranged from 0.9 $wt\%_{dry}$ (Ref_PL_a sample a) to 2.3 $wt\%_{dry}$ (K_FL_1.0 sample b). Notable variations were observed between samples a and b, particularly for Ref_FL, K_FL_0.8a, and K_FL_1.0, indicating greater fuel inhomogeneity on those days. The trials K_FL_0.3 and K_FL_0.8a, conducted on consecutive days (campaign #2), showed lower ash contents than the trials K_FL_0.8b and K_FL_1.0 (campaign #3). In the partial-load trials, the ash content of samples a and b was at similar levels for the respective trials. An increase in ash content with an increasing additive concentration was also observed, rising from an average of about 1.0 wt% in the reference trials to up to 2 wt%.

Due to the substantial variations between samples in all full-load trials, no clear correlation between increasing ash content and kaolin addition could be established here. The ash content exhibited high

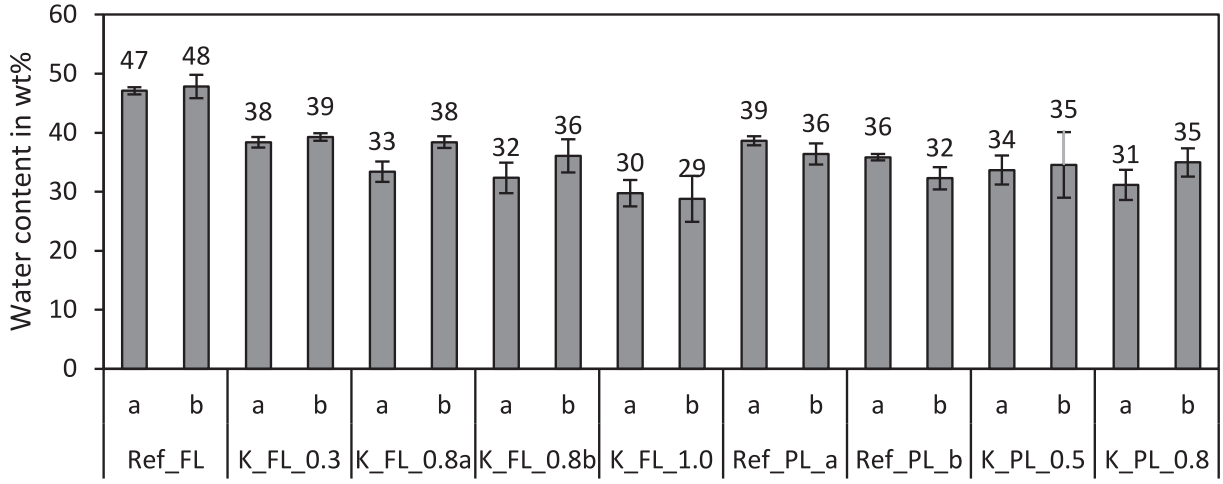

Fig. 3. Water content of (additivated) wood chip samples from the combustion in a large-scale CHP unit at full load (FL) and partial load (PL) operation without (Ref) and with the addition of 0.3 wt% (_0.3) till 1.0 wt% (_1.0) kaolin (K_). Samples were taken at the start (a) and at the end (b) of the total particulate matter measurements.

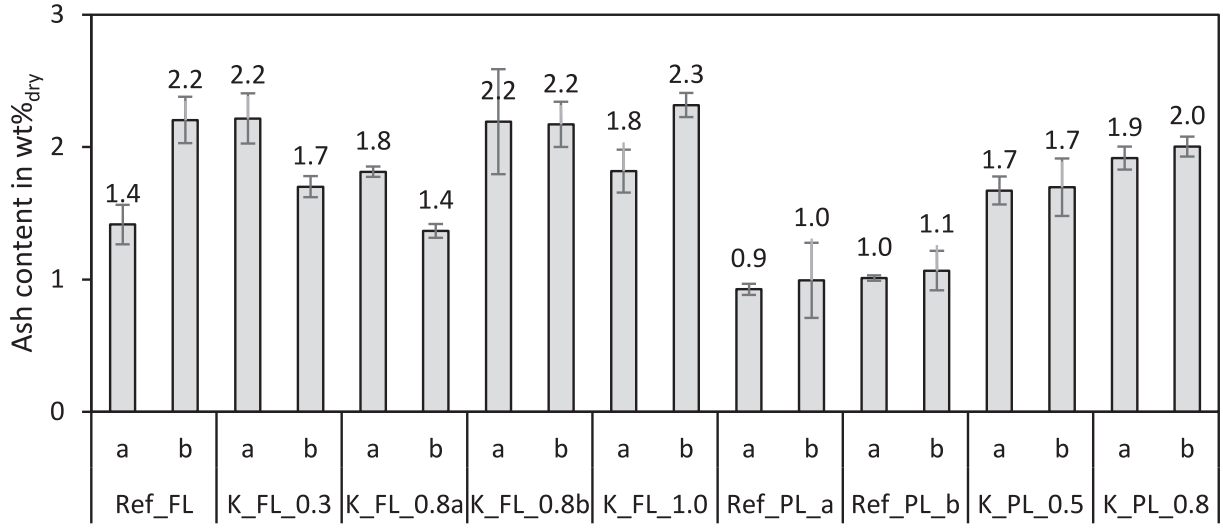

Fig. 4. Ash content of (additivated) wood chip samples from the combustion in a large-scale CHP unit at full load (FL) and partial load (PL) operation without (Ref) and with the addition of 0.3 wt% (_0.3) till 1.0 wt% (_1.0) kaolin (K_). Samples were taken at the start (a) and at the end (b) of the total particulate matter measurements.

fluctuations, both within individual trials and between trials, which complicate the comparability of the measured emissions. In contrast, the noticeable increase in ash content with additivation in the partial load trials can be attributed to the kaolin addition, elevating the measured ash fraction of the fuel. Assuming representative additivated fuel samples (e.g., a mean kaolin concentration of 0.5 wt% in the case of K_PL_0.5, both samples a and b), the intrinsic ash content of the biomass fuel (i.e., excluding the kaolin contribution) would correspond to ca. 1.2 $wt\%_{dry}$ for respective a and b samples for both K_PL_0.5 and K_PL_0.8. This suggests that the initial fuel had comparable ash contents across these partial load trials.

Chemical composition. The concentrations of potassium (K), calcium (Ca), sodium (Na), aluminum (Al), chloride (Cl^-), and sulfate (SO_4^{2-}) in the fuel are summarized in Table 3. In all samples, Ca constitutes the largest fraction of these components (maximum concentration of 4850 $mg_{Ca}/kg_{BM,dry}$ for K_FL_0.8b sample b), followed by K (maximum concentration of 2160 $mg_K/kg_{BM,dry}$ for Ref_FL sample b) and SO_4^{2-} (maximum concentration of 1460 $mg_{SO_4^{2-}}/kg_{BM,dry}$ for K_FL_1.0 sample a). The addition of kaolin increases Al concentrations in the fuel samples. In the reference cases, Al ranges from below the detection limit to 61 $mg_{Al}/kg_{BM,dry}$. In contrast, in most additivation cases the concentrations exceed 100 $mg_{Al}/kg_{BM,dry}$ and reach almost 600 $mg_{Al}/kg_{BM,dry}$ for sample K_FL_0.8b sample a. The concentrations of the remaining elements lie in the same order of magnitude across all cases, with average levels of 1600 $mg_K/kg_{BM,dry}$, 3225 $mg_{Ca}/kg_{BM,dry}$, 10 $mg_{Cl^-}/kg_{BM,dry}$, and 525 $mg_{SO_4^{2-}}/kg_{BM,dry}$, respectively, while Na averages around 262 $mg_{Na}/kg_{BM,dry}$. The observed fluctuations can be attributed to the inherent heterogeneity of the biomass feedstock, and no systematic influence of kaolin addition on these elements is evident.

A theoretical estimate – assuming a homogeneous kaolin distribution on the sampled fuel, an Al content of 18 wt% in kaolin and a fuel moisture content above 30 wt% – yields an expected additional 780 to 2600 $mg_{Al}/kg_{BM,dry}$ in the solid biofuel additivated with 0.3 to 1.0 wt% kaolin. The substantially lower measured values indicate that kaolin may be unevenly distributed on the biomass, partly due to temporal fluctuations in additive dosing caused by bridging in the big bags and partly because a fraction of the additive did not adhere to the fuel and visually cumulated in corners of the conveyor. Nonetheless, this may

Table 3
Chemical concentration of (additivated) wood chip samples from the combustion in a large-scale CHP unit at full load (FL) and partial load (PL) operation without (Ref) and with the addition of 0.3 wt% (_0.3) till 1.0 wt% (_1.0) kaolin (K_). Samples were taken at the start (a) and at the end (b) of the total particulate matter measurements.

Trial	Sample	K	Na	Al	Ca	Cl^-	SO_4^{2-}
		$mg/kg_{BM,dry}$					
Ref_FL	a	1798	41	51	3320	<40	786
	b	2159	56	61	4023	<53	834
K_FL_0.3	a	2150	66	296	4529	12	524
	b	1815	78	66	3128	8	300
K_FL_0.8a	a	1551	41	597	2692	7	404
	b	1508	54	415	3108	7	152
K_FL_0.8b	a	1415	53	382	3504	<10	740
	b	2039	<61	100	4874	<10	806
K_FL_1.0	a	2012	<47	<48	4046	<24	1458
	b	1955	<60	108	3865	<9	857
Ref_PL_a	a	1019	30	<50	2664	<10	349
	b	813	36	<28	2626	<10	363
Ref_PL_b	a	1292	27	36	2093	<10	249
	b	1486	40	32	2223	21	286
K_PL_0.5	a	1470	<47	346	2686	9	395
	b	1363	50	389	2800	8	299
K_PL_0.8	a	1258	42	504	2686	8	427
	b	1674	49	540	3184	10	222

have influenced the composition of the biomass samples, and thus the apparent additive-to-fuel ratio, more strongly than the actual kaolin input into the combustion chamber, since the conveyor turns upside down during fuel discharge, where additional mixing of additive and fuel is expected. The water content of the fuel potentially accelerated the formation of kaolin clumps, which accumulated in dead zones of the steep-chain conveyor or other handling equipment; thus, some of the additive may have been fully retained on the fuel sample.

3.2. Total particulate matter

Emissions. Fig. 5 presents the total particulate matter (TPM) emissions measured at the economizer during the additivation trials. In the reference full load trial, average total particulate matter concentrations were about 149 $mg/Nm^3_{6vol\%O2}$. In contrast, during partial-load operation, the reference cases yielded ca. 100 and 214 $mg/Nm^3_{6vol\%O2}$ for Ref_PL_a and Ref_PL_b, respectively, at steam loads of 28.4 t/h and 20.1 t/h (Table 2). Under full-load conditions, the average total particulate matter emissions were reduced by 17%, 30%, and 39% for kaolin addition rates of 0.8 (a), 0.8 (b), and 1.0 wt%, respectively, compared to the full-load reference. In the case of 0.3 wt% additivation, there was a slight (4%), but not significant, increase in median and average total particulate matter emissions. At partial load, the two reference trials showed differing emission levels, with total particulate matter concentrations of 100 $mg/Nm^3_{6vol\%O2}$ (Ref_PL_a) and 214 $mg/Nm^3_{6vol\%O2}$ (Ref_PL_b). Ref_PL_a exhibits the lowest total particulate matter levels of all trials. Depending on the chosen reference (Ref_PL_a or Ref_PL_b), the addition of 0.5 or 0.8 wt% kaolin either reduces total particulate matter by 37% and 39%, respectively, or increases it by 35% and 30%, respectively.

The biofuel in the full load reference case is characterized by a relatively higher moisture content representing a less favorable fuel condition and may therefore lead to higher emissions, potentially overestimating the effects of the additivation conducted with comparatively drier solid biofuel. Nevertheless, when considering the emissions and the mitigation achieved by kaolin addition in their overall context, it becomes evident that the trend of decreasing total particulate matter emissions with increasing kaolin concentrations is consistent. The relatively high standard deviations observed for the 1.0 wt% case in full load (K_FL_1.0) can be attributed to the fact that these tests were conducted with biofuels characterized by comparatively high ash content (Fig. 3), which implies poorer combustion properties and greater temporal fluctuations in emissions. The low particulate matter concentrations in Ref_PL_a are likely related to the low ash and K content in the fuel, which also limits its suitability as a representative reference state, whereas

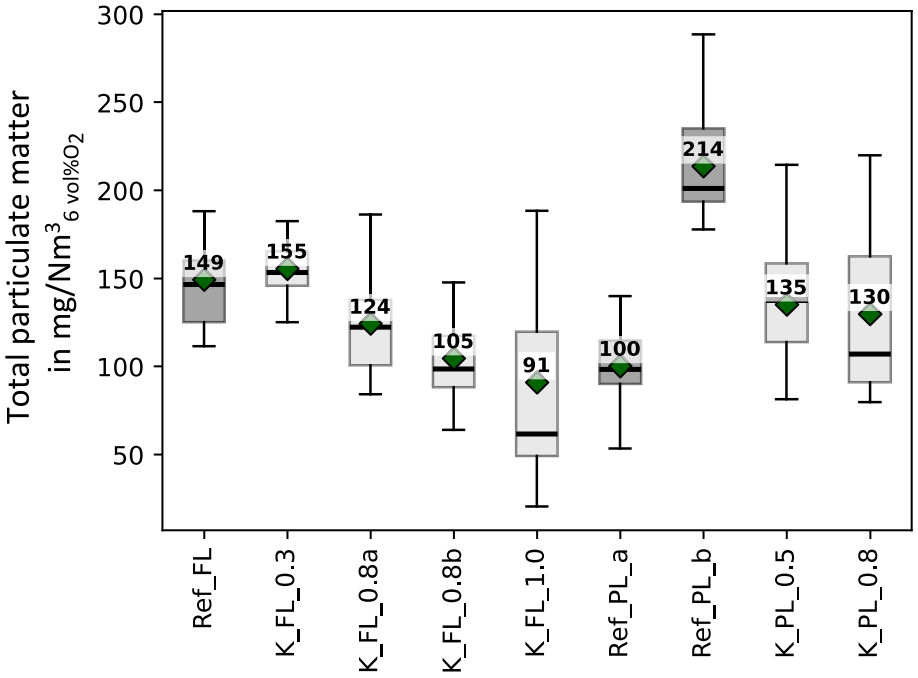

Fig. 5. Total particulate matter (TPM) emissions at the economizer (before cyclone and fabric filter) during the combustion of wood chips in a large-scale combined heat and power (CHP) unit at full load (FL) and partial load (PL) operation without (Ref) and with the addition of 0.3 wt% (_0.3) till 1.0 wt% (_1.0) kaolin (K_). Boxes span from quartile 25% (Q1) to 75% (Q3) (interquartile range IQR), line marks median, rhombus marks mean, whiskers cover the range of accepted values, reaching from box to datapoints within 1.5IQR: (minimum value without outliers < Q1–1.5xIQR, maximum value without outliers > Q3 + 1.5xIQR).

Ref_PL_b shows comparatively high emissions but also the lowest steam load. In terms of K content in the fuel, which is likely the primary aerosol source during biomass combustion, the fuel from Ref_PL_b shows comparable levels to the fuel samples from K_PL_0.5 and _0.8. In general, absolute emission-reduction levels remain difficult to compare due to variations in boiler load and aerosol forming elements within the biofuel, but decreasing total particulate matter levels with increasing additive concentration (particularly with similar K levels in the fuel), suggest that kaolin addition may mitigate emissions in both full and partial load operation.

Chemical composition. The concentrations of K, Ca, Na, Al, Cl^-, and SO_4^{2-} in the flue gas at the economizer, derived from the chemical composition of total particulate matter in the flue gas, are shown in Table 4. K and SO_4^{2-} dominate the chemical composition of total particulate matter, indicating that K_2SO_4 is a major particulate species in the flue gas. At the same time, Cl^-, Ca, and occasionally Al and Na occur only in minor amounts. With increasing kaolin additivation, both the relative and absolute K (and SO_4^{2-}) emissions in the flue gas decrease at full load, with absolute reductions in K of up to 73% for sample K_FL_0.8a, and at partial load, with absolute reductions of around 47% for K_PL_0.8 when referenced to Ref_PL_b. With Ref_PL_a as the reference, a relative reduction of about 20% in K concentration is still observed for 0.8 wt% kaolin, but the absolute K emissions increase by more than 30%.

Considering the K concentrations in the fuel (Table 3), Ref_PL_a had substantially lower average K levels than the other partial-load trials and therefore released less K (resulting in lower total particulate matter, as previously shown) into the gas phase, complicating any direct comparison of absolute emissions between these cases. Ca in biomass is mainly present as oxides, but also partly as carbonates, sulfates, or silicates, with high ash melting temperatures [28], therefore only to a limited extent detected in the flue gas. In contrast, K (and Na) is more volatile and is typically readily released to the gas phase during combustion, for example, as KCl and K_2SO_4, and partly as hydroxides such as KOH. These alkali species are a significant source of aerosols and precursors of fine particulate matter released with the flue gas into the atmosphere. In combination with silicon, K can form low-melting eutectic silicates [28]. In the presence of aluminosilicates, K can be incorporated into more stable, high-melting phases such as kalsilite ($KAlSiO_4$) and leucite ($KAlSi_2O_6$), thereby reducing its concentration in the flue gas, as observed here.

3.3. Bottom and cyclone ash

Bottom ash. Analogous to the fuel-sampling procedure, bottom ash (BA) samples were taken twice for each operating condition: sample (a) was collected before the start of total particulate matter measurements at the economizer (after the onset of additivation, where applicable), and sample (b) was collected after the final total particulate matter measurement.

In Table 5, the concentrations of K, Ca, Na, Al, Cl^-, and SO_4^{2-} in the bottom ash samples are summarized. The Ca concentration ranges from 84 to 204 $mg_{Ca}/kg_{BA,dry}$, with the highest value in K_FL_0.8b sample a and the lowest in K_FL_0.3 sample a, while K varies between 24 and 95 $mg_K/kg_{BA,dry}$, showing the highest value in the reference full-load case and the lowest values in the full-load trial with 1.0 wt% kaolin and in the Ref_PL_b sample a. Na, Cl^-, and SO_4^{2-} concentrations in bottom ash are negligible in most cases. Aluminum concentrations range from 3 $mg_{Al}/kg_{BA,dry}$ (Ref_FL sample b and K_FL_0.3 sample a) up to 33 $mg_{Al}/kg_{BA,dry}$ (K_PL_0.5 sample b). Except for K_PL_0.8, all b-samples – that is the bottom ash samples taken after completion of the total particulate matter measurements, when additivation had already been applied for several hours – exhibit higher Al concentrations than the corresponding a-samples, which originate from fuel with little (e.g., due to residues from previous days) or no additive.

No clear trend in K concentration attributable to kaolin addition is evident; the observed variations are more likely related to inhomogeneity and temporal fluctuations in the biomass feed, which also mask any theoretically expected increase in K retention in the bottom ash due to incorporation into kaolin-derived phases. At the same time, the addition of the additive dilutes the ash composition through increased Al and Si content, which may dilute the relative concentrations of K.

Fig. 6 shows the X-ray diffractograms of the bottom ash samples b for each trial, representing ash corresponding to the fuel present in the combustion chamber during total particulate matter sampling, after several hours of additivation. Peaks associated with Al-Si compounds are highlighted to visualize the formation of aluminosilicate phases. Under full load conditions, orthoclase reflections are visible in all cases, including the non-additivated reference, but their relative intensities tend to increase with kaolin addition. Leucite is clearly detectable only in additivated samples with kaolin dosages of at least 0.8 wt% at full load and 0.5 wt% at partial load, indicating enhanced formation of K-aluminosilicates at higher kaolin levels. Kalsilite is present in all trials, with the most pronounced peak observed for the K_FL_0.8 cases, whereas the diffractogram of K_FL_0.8b appears overall most amorphous. For the 1.0 wt% kaolin case, fewer distinct peaks are visible, but characteristic binding products can still be identified; since normalized intensities are shown, this is partly related to the dominance of a single, much sharper main peak. These observations confirm the formation of K-

Table 4
Chemical concentration in flue gas at the economizer (before cyclone and fabric filter) during the combustion of wood chips in a large-scale CHP unit at full load (FL) and partial load (PL) operation without (Ref) and with the addition of 0.3 wt% (_0.3) till 1.0 wt% (_1.0) kaolin (K_).

Trial	K	Na	Al	Ca	Cl^-	SO_4^{2-}
	$mg/Nm^3_{6\ vol\text{-}\%O2}$					
Ref_FL	107	3.1	2.4	5.9	4.9	51
K_FL_0.3	51	3.4	2.7	6.3	3.4	33
K_FL_0.8a	34	3.0	3.1	4.4	4.2	32
K_FL_0.8b	27	< 4.3	1.7	4.2	2.8	23
K_FL_1.0	40	< 4.8	1.5	17.7	2.6	24
Ref_PL_a	29	2.3	< 2.0	8.8	2.3	44
Ref_PL_b	70	4.1	< 3.0	7.0	5.7	76
K_PL_0.5	42	< 4.0	< 4.0	5.1	2.8	23
K_PL_0.8	37	< 5.0	< 5.0	11.0	2.6	24

Table 5
Chemical concentration in bottom ash (BA) samples from the combustion of wood chips in a large-scale CHP unit at full load (FL) and partial load (PL) operation without (Ref) and with the addition of 0.3°wt% (_0.3) till 1.0°wt% (_1.0) kaolin (K_). Samples were taken at start (a) and at the end (b) of the total particulate matter measurements.

Trial	Sample	K	Na	Al	Ca	Cl^-	SO_4^{2-}
		$mg/kg_{BA,dry}$					
Ref_FL	a	73	3,0	6,5	116	< 0,5	2,5
	b	95	3,5	3,3	125	< 0,5	1,4
K_FL_0.3	a	34	2,0	2,8	84	1,2	0,6
	b	46	2,5	8,4	91	1,5	0,7
K_FL_0.8a	a	49	2,6	7,3	121	1,3	0,7
	b	41	2,3	28,7	88	2,0	1,0
K_FL_0.8b	a	65	2,9	6,9	203	1,5	0,7
	b	70	3,0	25,6	197	1,1	0,5
K_FL_1.0	a	24	< 2,6	7,6	93	1,0	0,5
	b	48	< 2,6	9,1	150	2,7	1,7
Ref_PL_a	a	45	2,0	6,7	193	< 1,0	1,6
	b	48	3,1	7,0	182	< 1,1	1,5
Ref_PL_b	a	26	1,8	5,0	140	< 1,2	0,9
	b	32	2,5	7,3	130	< 1,3	1,3
K_PL_0.5	a	48	2,9	15,6	187	1,8	1,5
	b	57	2,9	32,6	172	1,0	1,2
K_PL_0.8	a	59	3,0	17,9	195	0,9	0,9
	b	49	3,2	15,9	160	0,8	0,8

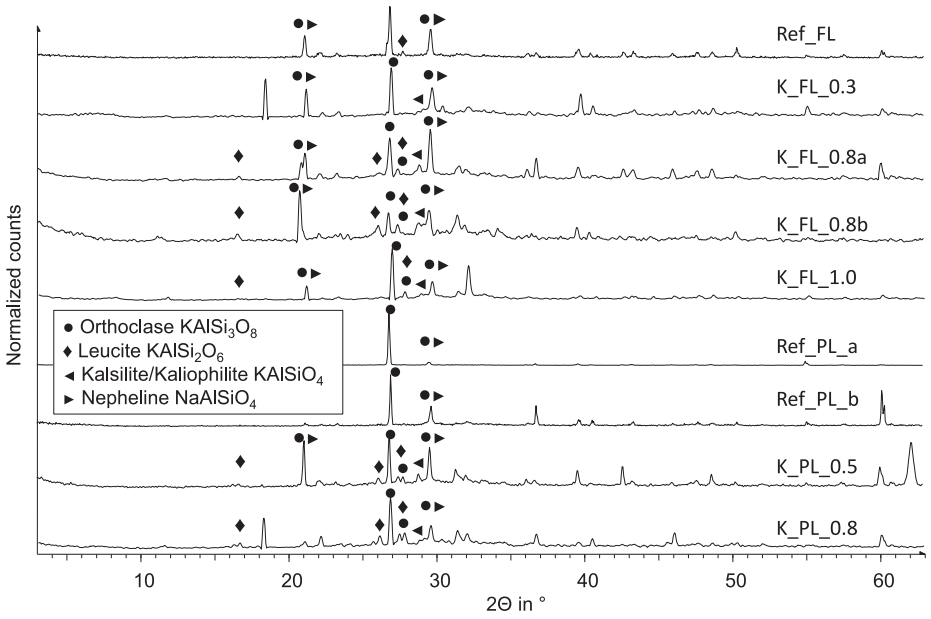

Fig. 6. X-ray diffractograms of bottom ash (sample b) of reference and additivation trials with detected crystalline phases containing Al and Si.

aluminosilicates in the additivation trials, providing evidence for K incorporation via reactions with kaolin in the bottom ash.

Cyclone ash. Cyclone ash (CA) was collected at the end of each of the six measurement campaigns and is therefore not available for every kaolin dosage trial. Table 6 summarizes the concentrations of K, Ca, Na, Al, Cl^-, and SO_4^{2-} in the cyclone ash samples. In the reference cases, K concentrations range from 47 and 56 $mg_K/kg_{CA,dry}$; in samples taken at the end of the additivation trials, these values are reduced by about 21% and 28% for 0.8 wt% and 1.0 wt% kaolin, respectively, at full load. Under partial load conditions, K concentrations are 26% or 34% lower for 0.8 wt% kaolin, depending on the selected reference case. Calcium concentrations in cyclone ash are also reduced in the additivated cases, although it is unclear whether this reduction is mainly due to variations in fuel composition or to kaolin addition itself. In contrast, Cl^- and SO_4^{2-} concentrations are higher in the additivated cases than in the non-additivated cases, contrary to trends reported for small-scale systems, where sulfate emissions typically decrease with kaolin addition [6,29].

In cyclones, the reduction of particulate matter addresses larger particle sizes than in fabric filters. Due to the plant design, collection of isolated fabric filter ash was not possible, although K concentrations and their mitigation potential in fabric filters are expected to be higher there, since, unlike Ca, K usually contributes to smaller particle sizes [30,31]. Nevertheless, a reduction of K concentrations could be established in the cyclone ash, consistent with reduced K emissions in the flue gas as discussed in chapter 3.2. Notably, Al concentrations in the cyclone also increase, which could be caused by kaolin particles entrained in the flue gas.

Table 6
Elemental concentration in cyclone ash (CA) samples from the combustion of wood chips in a large-scale CHP unit at full load (FL) and partial load (PL) operation without (Ref) and with the addition of 0.3 wt% (_0.3) till 1.0 wt% (_1.0) kaolin (K_).

Trial	K	Na	Al	Ca	Cl^-	SO_4^{2-}
	$mg/kg_{CA,dry}$					
Ref_FL	47	3.6	5.2	211	1.9	7
K_FL_0.8a	37	2.7	21.6	173	8.7	36
K_FL_1.0	34	< 2.8	28.4	129	1.5	26
Ref_PL_a	50	< 3.0	11.7	264	< 10	11
Ref_PL_b	56	3.7	6.3	259	4.8	27
K_PL_0.8	37	<2.9	17.5	132	2.6	42

3.4. Gaseous emissions

Fig. 7 shows the time course of CO emissions at the stack during the additivation trial with 0.8 wt% kaolin (trial b), chosen because no additive was dosed immediately before or after this period. Fig. 8 presents boxplots of CO and SO_2 emissions, Fig. 9 presents the emissions of NO_x and NH_3 during the reference and additivation trials. For the reference cases, the data underlying the boxplots for gaseous emissions correspond to the duration of the total particulate matter measurements. For the additivation trials, only data from at least 20 min after the start of kaolin dosing until its end were considered, as it takes some time for the additivated fuel to reach the combustion chamber. The last measurement point considered in the boxplots was 1 h after the end of kaolin dosing.

CO. Fig. 7 shows that, except for the first hours of the day and a few outliers coinciding with elevated CO emissions, the steam load remained nearly constant at 29 to 32 t/h throughout the day. The start of kaolin addition was at 11:00 am, and shortly thereafter, a marked decrease in CO emissions was observed, from about 20 to 25 $mg/Nm^3_{6vol\%O2}$ to a minimum of ca. 4 $mg/Nm^3_{6vol\%O2}$ around 2.5 h after the onset of dosing. Shortly after the end of kaolin addition, CO emissions increased again, although at midnight they remained slightly below the pre-kaolin additivation level. This may be attributed either to normal variability in average emissions or to residual additive on the conveyor that successively entered the combustion chamber and continued to reduce CO emissions slightly.

As shown in Fig. 8, the full load reference case shows an average CO concentration of 57 $mg/Nm^3_{6vol\%O2}$ with substantial variability as indicated by the whiskers of the boxplots. With kaolin addition, CO emissions are reduced by 21, 51, 84, and 91% for 0.3, 0.8 (a), 0.8 (b), and 1.0 wt% kaolin, respectively. In partial-load operation, and depending on the chosen reference (Ref_PL_a or Ref_PL_b), the addition of 0.5 and 0.8 wt% kaolin reduces CO emissions by 85% and 90% (relative to Ref_PL_a) or by 46% and 64% (relative to Ref_PL_b). Similar CO reductions due to kaolin additivation have been reported in literature [5,6,9,12,29,32]. As outlined in Section 1 and Fig. 1, potassium from the gas phase not only contributes to particulate matter emissions, but, as KCl and KOH it may lead to the inhibition of CO oxidation due to competitive reactions with radicals involved in gas phase oxidation [6]. The introduction of kaolin to the combustion chamber, leading to incorporation of K, therefore results in a mitigation of CO emissions. Absolute reduction levels,

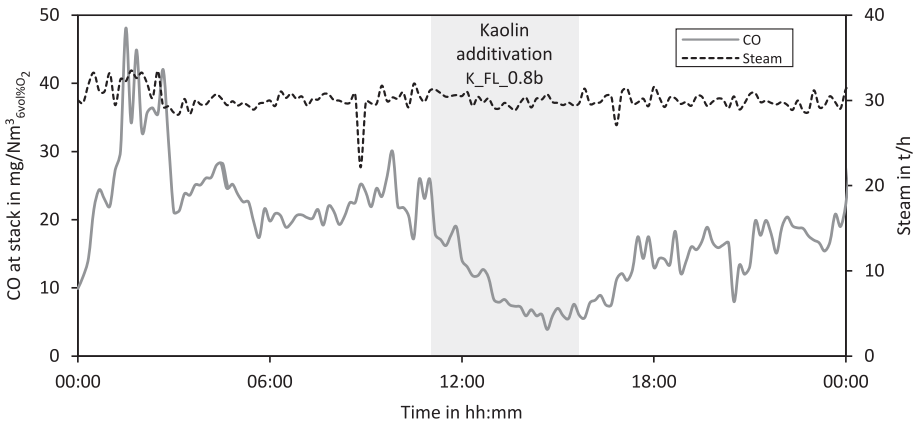

Fig. 7. CO emissions at the stack and steam amount over time on the day of kaolin additivation with 0.8 wt% (K_FL_0.8b). The time when kaolin was added is marked in grey.

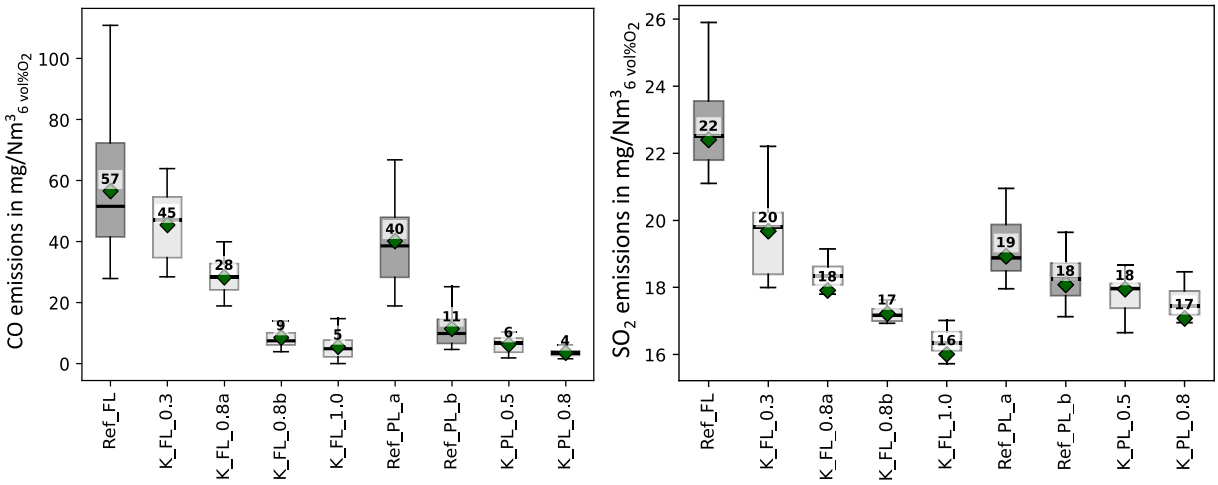

Fig. 8. CO emissions (left) and SO_2 emissions (right) in the flue gas from the combustion of wood chips in a large-scale CHP unit at full load (FL) and partial load (PL) operation without (Ref) and with the addition of 0.3 wt% (_0.3) till 1.0 wt% (_1.0) kaolin (K_). Boxes span from quartile 25% (Q1) to 75% (Q3) (interquartile range IQR), line marks median, rhombus marks mean, whiskers cover the range of accepted values, reaching from box to datapoints within 1.5IQR (minimum value without outliers < Q1–1.5xIQR, maximum value without outliers > Q3 + 1.5xIQR).

however, are only comparable with caution due to variations in boiler load and reference emission levels. When only the reference trials are considered (without accounting for fuel composition), CO concentrations tend to be higher at higher steam loads, implying that the reduction potential in K_FL_0.3 and K_FL_0.8a may be underestimated, while the reduction in partial-load trials relative to Ref_PL_a may be overestimated, and relative to Ref_PL_b may be underestimated.

SO_2. The emissions of SO_2 (Fig. 8) at full load operation are lower with kaolin additivation, i.e., from an average of 22 mg/$Nm^3_{6vol\%O2}$ (Ref_FL) to 16 mg/$Nm^3_{6vol\%O2}$ with 1.0 wt% kaolin (K_FL_1.0). In partial load, SO_2 emissions with kaolin were only slightly lower (average of 17 mg/$Nm^3_{6vol\%O2}$ with 0.8 wt% (K_PL_0.8) as opposed to 19 and 18 mg/$Nm^3_{6vol\%O2}$ in the reference cases (Ref_PL_a and Ref_PL_b)). This trend is contrasts with studies reporting increased SO_2 emissions with kaolin additivation [33,34], attributed to the reaction of kaolin with K-bearing species: K from K_2SO_4 is retained in the ash, whereas S is released as gas into the gas phase and then into the atmosphere – usually resulting in elevated SO_2 emissions. Other work, however, describes SO_2 adsorption or capture by (modified) kaolin, indicating that kaolin could also contribute to SO_2 reduction under certain conditions [35].

NO_x. NO_x emissions were measured at the stack, i.e., downstream of the SNCR system, and are therefore not suitable for isolating the effect of kaolin addition. Due to this, at full load, NO_x emissions do not show any systematic change with kaolin additivation (NO_x emissions under partial load conditions are not shown due to a chance of emissions thresholds and adjustment of urea dosage). However, the NH_3 slip from the SNCR system was lower in measurement trials with kaolin additivation. When urea ($(NH_2)_2CO$) is dosed into the plant, it breaks down into ammonia (NH_3) and fulminic acid (HCNO). NH_3 then reacts with available hydroxyl radicals ($^{\bullet}OH$) to form amine radicals ($^{\bullet}NH_2$), which then react with NO to form N_2 and water [36]. The reduction of NH_3 with kaolin additivation could therefore be a result of higher radical availability due to the reduced interference of KOH and KCl with the radical pool. Additionally, lower CO concentrations have been reported to shift selectivity due to increased local temperatures from CO oxidation [37].

3.5. Limitations

The experiments were subject to several limitations, particularly plant-specific conditions and fuel properties that may impede comparability between campaigns. The tests were conducted in an industrial power plant, which ensures district energy supply; however, due to load fluctuations, seasonal dependencies, and variations in fuel batches, identical experimental conditions could not be maintained across all test trials. These aspects are discussed in the following section and placed in context.

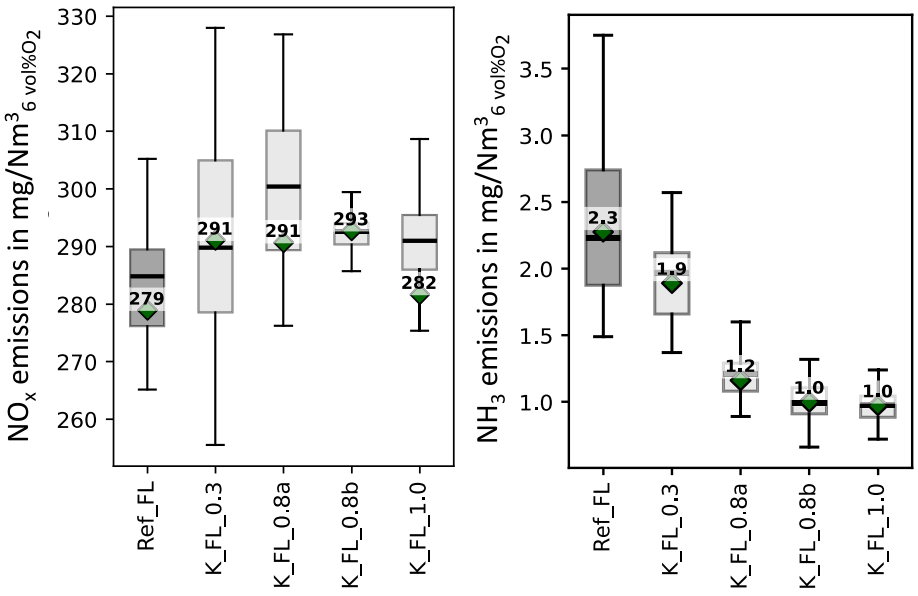

Fig. 9. NO_x emissions (left) and NH_3 emissions (right) in the flue gas from the combustion of wood chips in a large-scale CHP unit at full load (FL) and partial load (PL) operation without (Ref) and with the addition of 0.3 wt% (_0.3) till 1.0 wt% (_1.0) kaolin (K_). Boxes span from quartile 25% (Q1) to 75% (Q3) (interquartile range IQR), line marks median, rhombus marks mean, whiskers cover the range of accepted values, reaching from box to datapoints within 1.5IQR (minimum value without outliers < Q1–1.5xIQR, maximum value without outliers > Q3 + 1.5xIQR).

Timeline. The measurement campaigns spanned one year, although the full load measurements were completed within a few months: the reference campaign was in January 2025, K_FL_0.3 and _0.8a were conducted in March on two consecutive days, and K_FL_0.8b and _1.0 were conducted in May of the same year, also on two consecutive days. In contrast, the partial-load experiments were more widely spread, comprising reference trials in April and August 2024, followed by kaolin additivation trials K_PL_0.5 and K_PL_0.8 in April of the following year, with an outage between the two campaigns.

Steam load. Although the campaigns were classified as either partial load or full load, the actual steam load, particularly for partial-load experiments, varied considerably. This makes direct comparisons somewhat difficult, especially because it cannot be stated with certainty how load levels affect emissions. For CO emissions, the trend suggests higher emissions at higher load.

Fuel properties. Fuel properties, which strongly influence plant operation and emissions, also varied across all trials and campaigns. For example, high water content can lead to higher CO emissions [38], while high alkali contents (i.e., K and Na) in the biofuel support particulate matter formation and may inhibit CO oxidation [39].

In particular, in the full load campaigns, the relatively high water content of the biomass during the reference trial may have led to comparatively high CO emissions, which in turn may cause the CO reduction observed in the subsequent kaolin trials with lower fuel moisture to be overestimated. In the partial load campaigns, the moisture content was similar across all fuel samples, but steam load and K content differed significantly in the reference trials. In the Ref_PL_a campaign, the fuel samples showed relatively low K contents, which may explain the lower total particulate matter emissions compared with the other reference campaign and the additive trials. At the same time, the steam load was considerably higher than in the other partial-load campaigns, which may in turn explain the comparatively high CO emissions. If the reduction effects are referenced to Ref_PL_a, the CO reduction may therefore be overestimated, whereas the total particulate matter reduction may be underestimated. In the case of Ref_PL_b, the fuel properties were comparable, but the steam load was relatively low (20 t/h compared with 25.8 and 27.2 t/h in the additive trials), which may again have resulted in comparatively low CO emissions and thus an underestimation of the CO reduction attributable to kaolin.

The data from the experimental trials was evaluated and discussed based on the measured results, with reference to the corresponding reference campaigns/trials. Potential over- and underestimation effects are also addressed in the discussion above. Due to these variations, an additional comparison of day 1 and day 2 additivation trials within the respective measurement campaigns, where plant conditions (e.g., steam load) and fuel properties varied the least, are shown in Table 7. For all campaigns, the kaolin concentration on day 2 was higher than on day 1, and mean total particulate matter and CO emissions decreased with higher kaolin concentrations. The largest reduction on total particulate matter emissions, −20% between two days, was recorded for the highest difference in additive concentration (0.3 vs. 0.8 wt%, campaign #2), which also showed the highest absolute reduction in CO emissions from 45 to 28 $mg/Nm^3_{6\ vol\%O2}$ (highest relative CO reduction by 44% was within the trials in campaign #3).

4. Conclusion

Additivation trials in a 26 MW_{th} grate-fired biomass CHP unit showed reductions in carbon monoxide (CO) emissions at the stack and total particulate matter (TPM) emissions at the economizer with the addition of 0.3 to 1.0 wt% kaolin, both in full and in partial load operation. The chemical composition, as well as the water and ash content of the solid biofuel and the boiler load, varied significantly, complicating an absolute comparison, especially at partial load. Under full-load conditions the following reductions in flue gas emissions were measured: CO emissions decreased by 21, 51, 84, and 91% for kaolin dosages of 0.3, 0.8 (trial a), 0.8 (trial b), and 1.0 wt%, respectively while TPM emissions upstream of secondary mitigation measures decreased by 17, 30 and 39% for 0.8 (trial a), 0.8 (trial b), and 1.0 wt%, respectively.

The mitigation of potassium (K) in the flue gas, together with the formation of chemical compounds from kaolin and K embedded into the bottom ash, such as orthoclase, leucite, and kalsilite, as detected by XRD analyses of the ashes, additionally indicate the effectiveness of kaolin additivation. The chemical composition of cyclone ashes showed a slight reduction in K concentrations, while the bottom ash composition exhibited slightly higher Al concentrations due to the introduction of the aluminosilicate.

In contrast to literature on small-scale combustion units, SO_2

Table 7
Comparison of mean total particulate matter (TPM) and CO emissions, and the respective reduction within the days/trials of the same measurement campaign.

Campaign and month		Trial		TPM in $mg/Nm^3_{6\ vol\%O2}$			CO in $mg/Nm^3_{6\ vol\%O2}$		
		Day 1	Day 2	Day 1	Day 2		Day 1	Day 2	
#2	March 2025	K_FL_0.3	K_FL_0.8a	155	124	−20%	45	28	−38%
#3	May 2025	K_FL_0.8b	K_FL_1.0	105	91	−13%	9	5	−44%
#6	April 2025	K_PL_0.5	K_PL_0.8	135	130	−4%	6	4	−33%

concentrations decreased with the addition of kaolin, suggesting that, under the present S levels and operating conditions, kaolin does not promote additional SO_2 release but could even contribute to sulfur capture. While NO_x emissions are mainly influenced by the SNCR system, a reduction in NH_3 slip at the stack was observed. This could indicate – similar to the mechanisms leading to a reduction of CO emissions – a more favorable radical environment and potentially an improved utilization of the reducing agent. Further investigations should be conducted to confirm these results.

Overall, this study has shown that adding up to 1 wt% kaolin to wood chip combustion in a large-scale grate-fired combustion unit reduced CO, TPM, and K-based emissions in the flue gas. These results demonstrate that the kaolin additivation of (wood) fuels, which has been extensively investigated in small-scale combustion systems, may also be effective in large-scale combustion plants, despite the fact that the large-scale system exhibits higher inertia and involves a greater number of influencing parameters, which make the investigation and quantification of said effects more difficult.

Nevertheless, long-term effects, especially with a focus on long-term emission levels, ash compositions, and potential advantages in terms of corrosion and slagging, should still be investigated. Additionally, further options for kaolin addition to the fuel to should be considered for example by injecting the additive with the primary air directly into the combustion chamber.

CRediT authorship contribution statement

Theresa Siegmund: Writing – original draft, Visualization, Investigation, Conceptualization. **Lena Schultheiß:** Writing – review & editing, Investigation. **Martin Kaltschmitt:** Writing – review & editing, Supervision.

Funding

This project was funded by Deutsche Bundesstiftung Umwelt (DBU) (AZ 38675/01+02). Publishing fees supported by Funding Program Open Access Publishing of Hamburg University of Technology (TUHH).

Declaration of competing interest

The authors declare the following financial interests/personal relationships which may be considered as potential competing interests: Theresa Siegmund reports financial support was provided by German Federal Environmental Foundation. Martin Kaltschmitt reports a relationship with BEW Berliner Energie und Wärme that includes: consulting or advisory. If there are other authors, they declare that they have no known competing financial interests or personal relationships that could have appeared to influence the work reported in this paper.

Data availability

Data will be made available on request.

References

[1] S. van Loo, J. Koppejan, The handbook of biomass combustion and co-firing, Earthscan, London, 2008, https://doi.org/10.4324/9781849773041.
[2] T. Nussbaumer, Combustion and co-combustion of biomass: fundamentals, technologies, and primary measures for emission reduction, Energy Fuel 17 (2003) 1510–1521, https://doi.org/10.1021/ef030031q.
[3] A. Boriouchkine, A. Zakharov, S.-L. Jämsä-Jounela, Dynamic modeling of combustion in a BioGrate furnace: the effect of operation parameters on biomass firing, Chem. Eng. Sci. 69 (2012) 669–678, https://doi.org/10.1016/j.ces.2011.11.032.
[4] R. Singh, A. Shukla, A review on methods of flue gas cleaning from combustion of biomass, Renew. Sust. Energ. Rev. 29 (2014) 854–864, https://doi.org/10.1016/j.rser.2013.09.005.
[5] J.L. Míguez, J. Porteiro, F. Behrendt, D. Blanco, D. Patiño, A. Dieguez-Alonso, Review of the use of additives to mitigate operational problems associated with the combustion of biomass with high content in ash-forming species, Renew. Sust. Energ. Rev. 141 (2021) 110502, https://doi.org/10.1016/j.rser.2020.110502.
[6] T. Siegmund, C. Gollmer, M. Scherzinger, M. Kaltschmitt, A review of CO emissions during solid biofuel combustion – formation mechanisms and fuel-related reduction measures, J. Energy Inst. 116 (2024) 101762, https://doi.org/10.1016/j.joei.2024.101762.
[7] J.-E. Eriksson, J. Lehmusto, L. Silvander, D. Lindberg, M. Zevenhoven, P. Yrjas, A. Brink, M. Hupa, L. Hupa, Corrosion of heat-transfer materials induced by KCl, HCl, and O2 under chemical-looping conditions, High Temp. Corros. Mater. (2024), https://doi.org/10.1007/s11085-024-10250-1.
[8] L. Wang, J.E. Hustad, Ø. Skreiberg, G. Skjevrak, M. Grønli, A critical review on additives to reduce ash related operation problems in biomass combustion applications, Energy Procedia 20 (2012) 20–29, https://doi.org/10.1016/j.egypro.2012.03.004.
[9] R. Mack, D. Kuptz, C. Schön, H. Hartmann, Combustion behavior and slagging tendencies of kaolin additivated agricultural pellets and of wood-straw pellet blends in a small-scale boiler, Biomass Bioenergy 125 (2019) 50–62, https://doi.org/10.1016/j.biombioe.2019.04.003.
[10] I. Höfer, T. Huelsmann, M. Kaltschmitt, Influence of Ca- and Al-additives on the pollutant emissions from blends of wood and straw in small-scale combustion, Biomass Bioenergy 150 (2021) 106135, https://doi.org/10.1016/j.biombioe.2021.106135.
[11] M. Gehrig, M. Wöhler, S. Pelz, J. Steinbrink, H. Thorwarth, Kaolin as additive in wood pellet combustion with several mixtures of spruce and short-rotation-coppice willow and its influence on emissions and ashes, Fuel 235 (2019) 610–616, https://doi.org/10.1016/j.fuel.2018.08.028.
[12] L.S. Bäfver, M. Rönnbäck, B. Leckner, F. Claesson, C. Tullin, Particle emission from combustion of oat grain and its potential reduction by addition of limestone or kaolin, Fuel Process. Technol. 90 (2009) 353–359, https://doi.org/10.1016/j.fuproc.2008.10.006.
[13] S. Xiong, J. Burvall, H. Örberg, G. Kalen, M. Thyrel, M. Öhman, D. Boström, Slagging characteristics during combustion of corn stovers with and without Kaolin and Calcite, Energy Fuel 22 (2008) 3465–3470, https://doi.org/10.1021/ef700718j.
[14] K.O. Davidsson, L.-E. Åmand, B.-M. Steenari, A.-L. Elled, D. Eskilsson, B. Leckner, Countermeasures against alkali-related problems during combustion of biomass in a circulating fluidized bed boiler, Chem. Eng. Sci. 63 (2008) 5314–5329, https://doi.org/10.1016/j.ces.2008.07.012.
[15] K.O. Davidsson, B.-M. Steenari, D. Eskilsson, Kaolin addition during biomass combustion in a 35 MW circulating fluidized-bed boiler, Energy Fuel 21 (2007) 1959–1966, https://doi.org/10.1021/ef070055n.
[16] B.-M. Steenari, K. Karlfeldt Fedje, Addition of kaolin as potassium sorbent in the combustion of wood fuel – effects on fly ash properties, Fuel 89 (2010) 2026–2032, https://doi.org/10.1016/j.fuel.2010.02.006.
[17] J.H. Zeuthen, P.A. Jensen, J.P. Jensen, H. Livbjerg, Aerosol formation during the combustion of straw with addition of sorbents, Energy Fuel 21 (2007) 699–709, https://doi.org/10.1021/ef060392g.
[18] L. Tobiasen, R. Skytte, L.S. Pedersen, S.T. Pedersen, M.A. Lindberg, Deposit characteristic after injection of additives to a Danish straw-fired suspension boiler, Fuel Process. Technol. 88 (2007) 1108–1117, https://doi.org/10.1016/j.fuproc.2007.06.017.
[19] Bundesrepublik Deutschland, Bundesministerium für Justiz, Bundesamt für Justiz, Vierundvierzigste Verordnung zur Durchführung des Bundes-Immissionsschutzgesetzes (Verordnung über mittelgroße Feuerungs-, Gasturbinen- und Verbrennungsmotoranlagen - 44. BImSchV) (German). https://www.gesetze-im-internet.de/bimschv_44/BJNR080410019.html, 2019 (accessed September 2, 2026).
[20] Gebrüder Dorfner GmbH Co, Kaolin- Uund Kristallquarzsandwerke KG, Technical Data Sheet: Kaolin FP 80, Ground, Hirschau, Germany, 2016.
[21] Deutsches Institut für Normung e.V (Ed.), DIN EN ISO 16967 Solid biofuels - Determination of major elements Al, Ca, Fe, Mg, P, K, Si, Na and Ti, 2015.

[22] Deutsches Institut für Normung e.V (Ed.), DIN EN ISO 18122 Solid biofuels - Determination of ash content, 2015.
[23] DIN 22022-1, Solid Fuels – Determination of Contents of Trace Elements – Part 1: General Rules, Sampling and Sample Preparation – Preparation of Samples for the Analyses (Dissolution Method), Deutsches Institut für Normung e.V, 2014.
[24] DIN EN ISO 10304-1, Water Quality – Determination of Dissolved Anions by Liquid Chromatography of Ions – Part 1: Determination of Bromide, Chloride, Fluoride, Nitrate, Nitrite, Phosphate and Sulfate, Deutsches Institut für Normung e.V, 2009.
[25] B.M. Jenkins, L.L. Baxter, T.R.M. Jr, T.R. Miles, Combustion Properties of Biomass, 1998, https://doi.org/10.1016/S0378-3820(97)00059-3.
[26] M. Lieskovský, M. Jankovský, M. Trenčiansky, J. Merganič, Ash content vs. the economics of using wood chips for energy: model based on data from Central Europe, BioResources 12 (2017) 1579–1592, https://doi.org/10.15376/biores.12.1.1579-1592.
[27] N. Pedišius, M. Praspaliauskas, J. Pedišius, E.F. Dzenajavičienė, Analysis of wood chip characteristics for energy production in Lithuania, Energies 14 (2021) 3931, https://doi.org/10.3390/en14133931.
[28] S.V. Vassilev, D. Baxter, C.G. Vassileva, An overview of the behaviour of biomass during combustion: part I. Phase-mineral transformations of organic and inorganic matter, Fuel 112 (2013) 391–449, https://doi.org/10.1016/j.fuel.2013.05.043.
[29] C. Gollmer, V. Weigel, M. Kaltschmitt, Emission mitigation by aluminum-silicate-based fuel additivation of wood chips with kaolin and kaolinite, Energies 16 (2023) 3095, https://doi.org/10.3390/en16073095.
[30] W. Yang, Y. Zhu, W. Cheng, H. Sang, H. Yang, H. Chen, Characteristics of particulate matter emitted from agricultural biomass combustion, Energy Fuel 31 (2017) 7493–7501, https://doi.org/10.1021/acs.energyfuels.7b00229.
[31] X. Liu, M. Xu, H. Yao, D. Yu, X. Gao, Q. Cao, Y. Cai, Effect of combustion parameters on the emission and chemical composition of particulate matter during coal combustion, Energy Fuel 21 (2007) 157–162, https://doi.org/10.1021/ef060324u.
[32] T. Siegmund, C. Gollmer, N. Horstmann, M. Kaltschmitt, Carbon monoxide (CO) and particulate matter (PM) emissions during the combustion of wood pellets in a small-scale combustion unit – Influence of aluminum-(silicate-)based fuel additivation, Fuel Process. Technol. (2024), https://doi.org/10.1016/j.fuproc.2024.108111.
[33] K.J. Wolf, A. Smeda, M. Müller, K. Hilpert, Investigations on the influence of additives for SO_2 reduction during high alkaline biomass combustion, Energy Fuel 19 (2005) 820–824, https://doi.org/10.1021/ef040081a.
[34] R. Mack, D. Kuptz, C. Schön, H. Hartmann, TFZ-Bericht 65 - Schwierige Pelletbrennstoffe für Kleinfeuerungsanlagen - Verbrennungstechnische Optimierung durch Additivierung und Mischung (German), Straubing, 2020.
[35] C. Volzone, J. Ortiga, SO2 gas adsorption by modified kaolin clays: influence of previous heating and time acid treatments, J. Environ. Manag. 92 (2011) 2590–2595, https://doi.org/10.1016/j.jenvman.2011.05.031.
[36] J.L. Sorrels, D.D. Randall, C.R. Fry, K.S. Schaffner, Chapter 1 - Selective Noncatalytic Reduction. https://www.epa.gov/sites/default/files/2017-12/documents/sncrcostmanualchapter7thedition20162017revisions.pdf, 2019 (accessed May 8, 2026).
[37] T. Blejchař, J. Konvička, B. Von Der Heide, R. Malý, M. Maier, High Temperature Modification of SNCR Technology and its Impact on NOx Removal Process, EPJ Web Conf. 180 (2018), https://doi.org/10.1051/epjconf/201818002009.
[38] Y.B. Yang, V.N. Sharifi, J. Swithenbank, Effect of air flow rate and fuel moisture on the burning behaviours of biomass and simulated municipal solid wastes in packed beds, Fuel 83 (2004) 1553–1562, https://doi.org/10.1016/j.fuel.2004.01.016.
[39] A. Chanpirak, H. Wu, P. Glarborg, P. Marshall, An experimental and chemical kinetic modeling study of the role of potassium in the moist oxidation of CO, Fuel 335 (2023) 127075, https://doi.org/10.1016/j.fuel.2022.127075.